Hindawi
Shock and Vibration
Volume 2023, Article ID 7288450, 20 pages
https://doi.org/10.1155/2023/7288450

Research Article

Seismic Behaviour of Multistorey Steel Framed Tall Buildings Using Intentionally Eccentric Braces

Nima Gholizadeh and Feng Fu

Department of Engineering, School of Science and Technology, City, University of London, EC1V 0HB, London, UK

Correspondence should be addressed to Feng Fu; feng.fu.1@city.ac.uk

Received 12 October 2021; Revised 1 March 2022; Accepted 2 May 2023; Published 21 June 2023

Academic Editor: Ehsan Ahmadi

Braces with intentional eccentricity (BIE) are recently proposed to improve the seismic behaviour of conventional buckling braces (CBBs) by inserting intentional eccentricity along the brace length. Due to this eccentricity and the resultant bending moment, the BIE bends uniformly from small storey drifts and moves smoothly into the postbuckling behaviour under compression and sustains trilinear behaviour under tension. This behaviour delays the appearance of midlength local buckling which causes unstable energy dissipation. BIEs have a desirable postyielding stiffness which results in stable energy dissipation during cyclic loading and are capable of dissipating energy during low-intensity earthquakes. The seismic behaviour of structures with BIEs for use in buildings has not yet been investigated, specifically in tall buildings. Therefore, this study concentrates on investigating the seismic behaviour of tall buildings equipped with BIEs that uses a 3-dimensional (3D) finite element model in ETABS. In the first step, a 20-storey structure is designed using both eccentric brace frame (EBF) and BIE system and their seismic performance under the TABAS earthquake record is compared. In the second step, the seismic performance of a 25-storey irregular structure is assessed to evaluate the efficiency of the BIE system in irregular structures. Results show the desirable performance and energy dissipation capacity of the BIE system but it also shows large out-of-plane deformation in some cases.

1. Introduction

Bracing systems are widely used as lateral resisting systems in various types of low-rise and tall buildings. Bracing is an efficient and economical method to provide stiffness and strength against lateral loads. Its efficiency is mainly because of the fact that the diagonal members work primarily in the axial stress, so that minimum member sizes are required in the structural systems. Concentric bracing and eccentric bracing are the two major categories of bracing.

The typical concentrically braced frames (CBFs) can only take axial loading in the braces. In a concentric bracing system, all of the members (beams, columns, and bracing) are oriented in a manner that all of them meet at a common point [1]. One of the main disadvantages of CBFs is their unreliable behaviour under cyclic loading. On the other hand, the energy dissipation mechanism is not quite efficient in concentrically braced frames [2–4]. As another disadvantage of CBFs, many experimental studies have revealed that because of the rapid increase in concentrated plastic strain, fracture follows the local buckling of concentric braces.

In eccentric bracings (EBFs), both axial loading members and bending members (the horizontal members) are involved in the lateral load-carrying mechanism. In eccentric bracing, the braces are placed with an offset from the columns. Eccentric bracing can provide the advantages of concentric bracing, while it has a significant ductility. On the other hand, in the context of architectural considerations, EBFs may provide larger openings in braced spans. However, the required detailing in EBFs is much more complicated than the concentric bracing [5].

The postyielding stiffness is one of the behavioural parameters that affect the structural response besides the strength, stiffness, and ductility. The high postyielding stiffness of structures results in a larger amount of energy

being absorbed during seismic excitation [6] and also less seismic demand in terms of strength and residual displacement [7]. The load-displacement relationship of structural systems with high postyielding stiffness may be characterized by trilinear behaviour which better satisfies the multilevel seismic design criteria [8]. In addition, larger postyielding stiffness results in a reduction in residual displacement demand of structures and help to prevent the soft-storey mechanism [9]. While conventional bracings provide limited postyielding stiffness, it, however, enhances the aforementioned weaknesses of CBFs which may be considered a motivation for developing new steel bracing systems.

Recently a new design of bracings has been introduced to improve the seismic performance of braced structures by controlling important structural characteristics, such as the initial stiffness, yield strength, the drift at which the system starts to dissipate energy, the postyielding stiffness, the local buckling concentration, the total dissipated energy, and the drift at which fracture occurs. In this newly introduced bracing named as braces with intentional eccentricity (BIE), an intentional eccentricity is inserted along the brace length which controls the brace deformation.

The first outstanding research work on BIEs was carried out by Skalomenos et al. [10]. They proposed a prototype design of conventional buckling braces by introducing an initial eccentricity along the brace length which results in an improved seismic performance. In their experimental work, five half-scaled BIE specimens were tested under a cyclic lateral load protocol for drift angles ranging from 0.10 to 4.0%. Also, they tested a conventional brace specimen with identical dimensions and zero eccentricity under the same loading pattern to conduct a comparative study. Their results showed the capability of the proposed steel brace in enhancing some of the negative traits of conventional steel brace. They concluded that their proposed bracing system may be considered as a viable alternative for steel bracings.

Skalomenos et al. [10] developed an online hybrid test environment to assess the seismic performance of the gusset plate connections of steel braces. In this regard, they incorporated substructuring techniques and finite element methods. Skalomenos et al. [11] presented an experimental investigation on the material properties of induction heat (IH) treated with steel elements used in BIEs. They used IH treatment and applied it to one-half of the cross-section to enhance the strength of that part, while the remaining part had the conventional properties of steel. Their tests showed that the treated brace exhibits a high postyielding tensile stiffness (equal to 20% of the initial stiffness). Also, the specimen was capable of dissipating energy during cyclic loading up to 2.0% storey drift because of the considerable delay in local buckling.

González Ureña et al. [12] used a procedure based on the direct displacement-based design (DDBD) method for the seismic design of 2D frames with BIEs. By using this method, they designed buildings with 4, 8, and 12 storeys. BIEs were assumed to be of HSS sections with target drift ratios of 1.5% and 2.5%. They also designed the same buildings with special CBFs to provide a comparative study. Their results showed that the design procedure they employed was suitable for the design of BIEs. They assessed the seismic performance of the structures and concluded that BIEs may provide an economically efficient alternative to conventional CBFs.

While the abovementioned experimental and analytical research works have been carried out on the cyclic behaviour of this type of braces on the element level, the global behaviour of structures equipped with these bracings has not yet been assessed, especially for tall buildings. Therefore, this research aims at investigating the seismic behaviour of tall steel structures equipped with BIEs under earthquake records and comparing its energy dissipation capacity with the EBF system. The 3-dimensional (3D) finite element models in ETABS will be used to provide a detailed understanding of the structural responses.

Response-history analyses are performed using ETABS to assess the seismic performance of the structure. The storey drifts, base shear, and dissipated energy are assessed using the responses under the TABAS earthquake record. The cyclic behaviour of BIEs is also assessed.

2. Braces with Intentional Eccentricity (BIE)

In braces with intentional eccentricity (BIE), as shown in Figure 1, an intentional eccentricity e is introduced along the brace length which affects the deformation of the brace. With this eccentricity, BIEs undergo overall bending with a small storey drift. Figure 2 shows the deformed shape of a BIE. The moment generated by the eccentrically applied axial force results in more uniformly distributed stresses and strains along the brace length. This delays the local buckling concentration resulting in extended ductile behaviour of the brace element.

The cyclic behaviour of BIEs is the main aspect of these bracing systems which affects the global behaviour of the structure under seismic loadings. Since ETABS will be used to analyse the structure and acquire the structural responses under earthquake records, a proper model of the BIE should be developed in ETABS. This model should be verified by the results from previous studies to attain a proper estimate of the BIE's cyclic behaviour and backbone curve.

The first step in modelling the BIE system in structures is developing a model of the brace at the element level. A beam element with fiber hinges is used here to model the flexural behaviour and an axial hinge is used to model the axial behaviour of the element. These hinges are modelled in parallel and placed at the middle and two ends of the

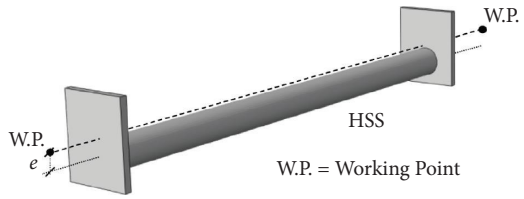

Figure 1: Configuration of the BIE [10].

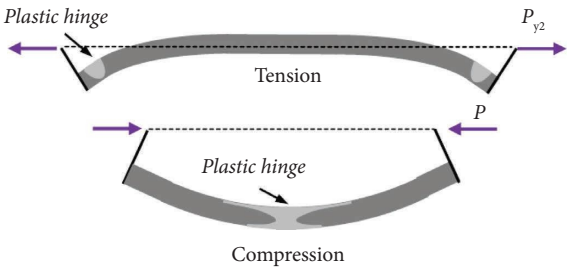

Figure 2: Deformed shape of brace under tensile and compressive loads [13].

element. The generated model in ETABS is shown in Figure 3. As can be seen in the figure, the eccentricity is imposed via the rigid links at the two ends of the element.

The fiber hinges are modelled using 10 layers in each direction of the section. This fiber section is shown in Figure 4. It is assumed that the brace bends only in the out-of-plane direction.

2.1. Axial Loading. In order to verify the developed model in ETABS, the results obtained in a work by González Ureña et al. [12] are studied here. They used OpenSees to model BIEs and to assess their behaviour and the effects of the different parameters. Their model was verified by the experimental results of Skalomenos et al. [14] and also the shell-based finite element models in the commercial software, Abaqus. The load-displacement behaviour of an element in tension and compression is reported in their work for a HSS $178 \times 178 \times 16$ with a 5408 mm long modelled. A nominal yield stress of 345 MPa was considered for the HSS section. A displacement control loading is performed by ETABS in this study. An axial load is exerted on the element in the left end, while the right end is constrained and 100 mm displacement in compression and 250 mm displacement in tension is applied to the element. The cross-sections and rigid elements are also shown in Figure 5.

A deformed shape of the element in compression is shown in Figure 6 in a step with a 100 mm displacement and in tension with a 126.9 mm displacement as shown in Figure 7.

Under compression, the axial hinge remains in its elastic state while the fiber hinge bends considerably. In tension, both tension and flexure contribute to the load-displacement diagrams. To verify the behaviour of the developed model, the load-displacement diagrams generated by González Ureña et al. [12] are compared with the results of the generated model in this study as shown in Figure 8. In the figure, the dashed lines are the results obtained from the model generated in this study. It can be seen that the developed model succeeds in providing good estimates of the compressive and tensile behaviour of BIE.

2.2. Cyclic Behaviour. Furthermore, the cyclic behaviour of the element is verified. In the work by González Ureña et al. [12], the axial force vs. lateral drift hysteretic plots of the same HSS element with an eccentricity of 180 mm were generated. They used OpenSees to analyse a braced bay with a 6 m width and 4 m height. The loading protocol had symmetrical cycles of increasing equivalent storey drifts of 0.1, 0.25, 0.75, 1.0, 1.5, 2, and 3%. As expected, the BIE showed a significant postyield stiffness in tension, in contrast with the CCB. In the compression stage, the BIE exhibited a stabilized maximum load equal to the postbuckling force.

The single element developed in the previous part is assembled in a frame with $e = 180$ mm eccentricity and the dimensions stated above as shown in Figure 9. A cyclic loading is applied to the upper node of the frame.

A displacement loading protocol is applied to the left-most upper node of the frame as shown in Figure 10.

The load-displacement diagram of the frame is verified with the results of González Ureña et al. [12] as shown in Figure 11. The blue line in the figure is the result obtained by the model developed in this study using ETABS. As can be seen, a good agreement is achieved in this model. It should be noted that the difference in these two results may be caused by the different assumptions in the degrading parameters of the two models.

The nonlinear moment-rotation behaviour of the hinge at the middle of the brace is shown in Figure 12. Based on the verification in this section, the developed element model will be used in the structural model to assess the seismic performance of the structures with BIEs.

3. 20-Storey Structure

3.1. EBF System. The first structural model for which the seismic performance will be assessed is a 20-storey building in an area with high seismicity. Eurocodes 3 and 8 are used to design the structure. It is assumed that the ground type is B and the seismic zone is 1 with $a_{gr} = 0.35$ g according to [15]. The storey heights are 3.5 m and the bay widths are 6 m. Steel materials are assumed to have a yield stress of 345 MPa. A 3D layout of the frame is shown in Figure 13. To make a comparative study, the structure is first designed by the EBF system while all beam to column connections including link beam to column connections are hinged.

3.2. Horizontal Elastic Response Spectrum. According to the seismic parameters for the location of the building, the horizontal elastic response spectrum will be calculated according to Eurocode 8 [16]. Here, we have $S = 1.2$, $T_B(s) = 0.15$, $T_C(s) = 0.5$, $T_D(s) = 2.0$, and $\eta = \sqrt{10/(5+\xi)} = 1, \xi = 5\%$. Therefore, the elastic response spectrum will be calculated as shown in Figure 14.

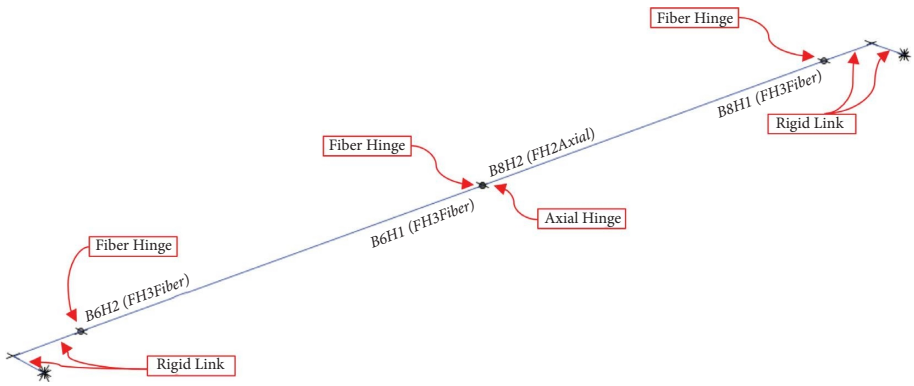

Figure 3: Flexural and axial hinges in the BIE element.

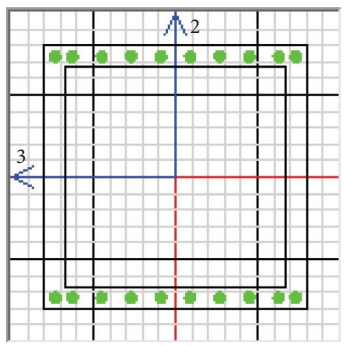

Figure 4: Fiber section for HSS 178 × 178 × 16.

Figure 5: Schematics of the element.

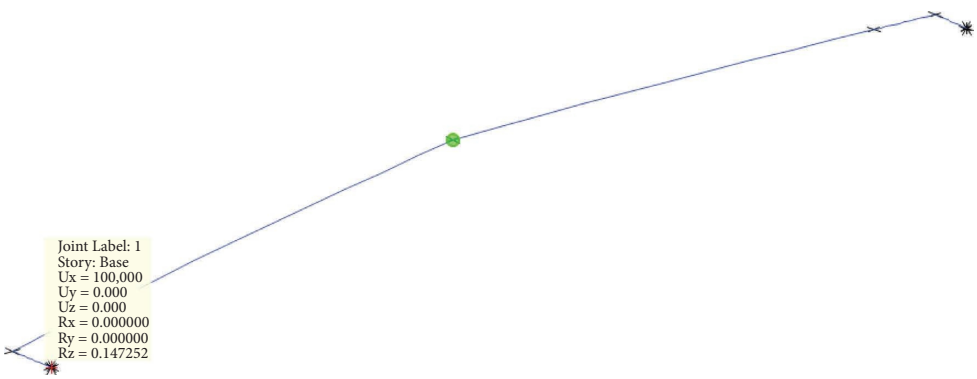

Figure 6: Deformed shape of the element in compression delta = 100 mm.

For the purpose of elastic design of the structure, the behaviour factor should be calculated. According to Eurocode 8 [16], the behaviour factor for the DCH ductility class and frame with eccentric bracings would be $5\alpha_u/\alpha_1$, while the value of α_u/α_1 is 1.2. Hence, the value of the behaviour factor is obtained as $q = 6$, and therefore, the design

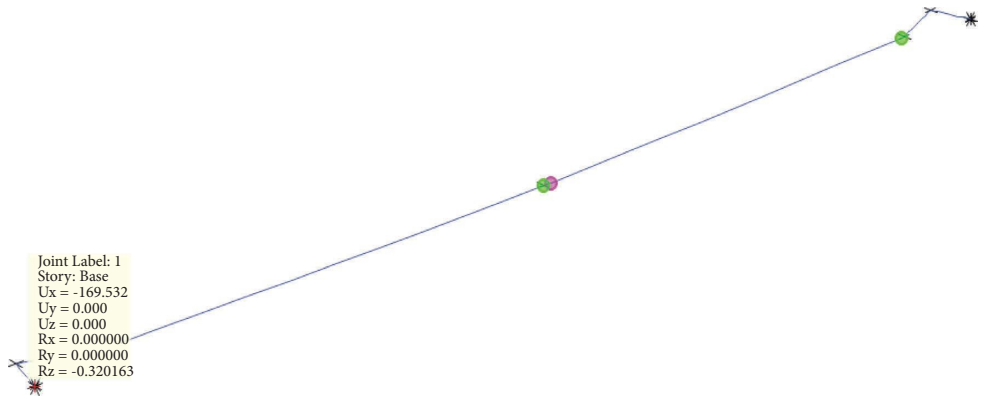

Figure 7: Deformed shape of the element in tension delta = 126.9 mm.

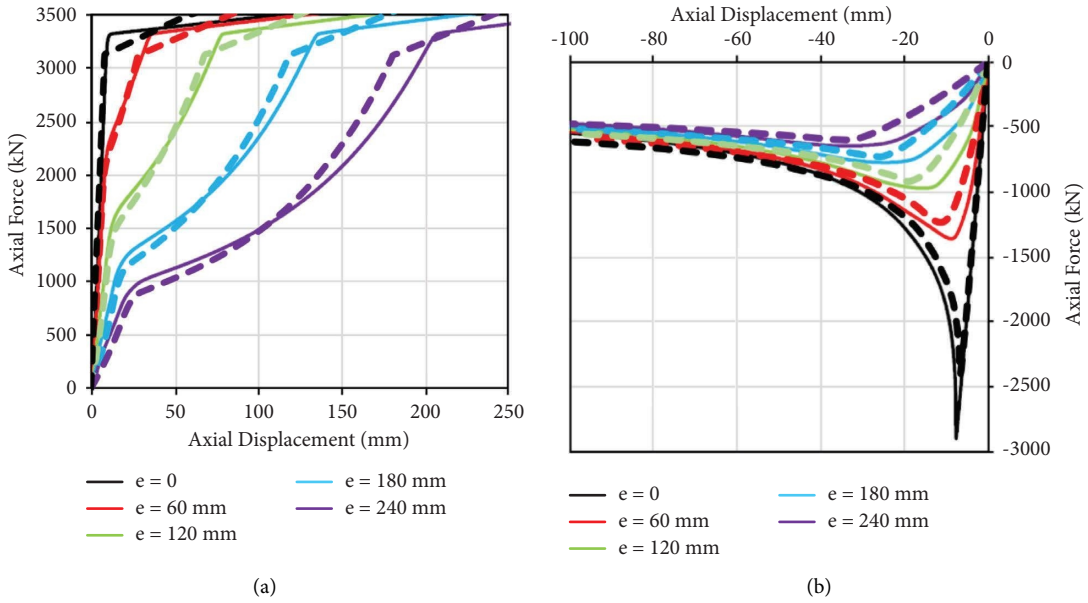

Figure 8: Comparison of the load-displacement diagrams generated by González Ureña et al. [12] with the results of the generated model in this study for a HSS 178 × 178 × 16 BIEs with $L = 5408$ mm and Lea = 360 mm: tension (a) and (b) compression.

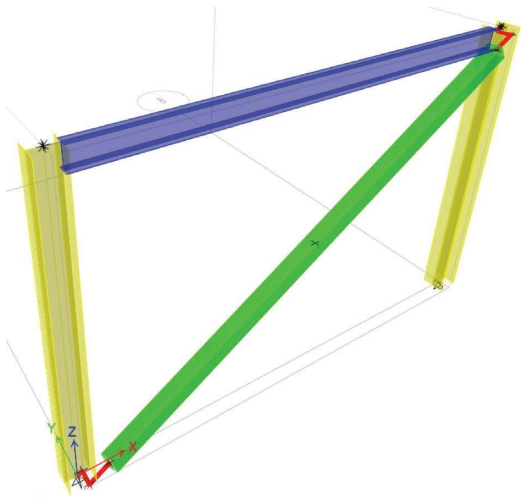

Figure 9: The frame with BIE element with $e = 180$ mm.

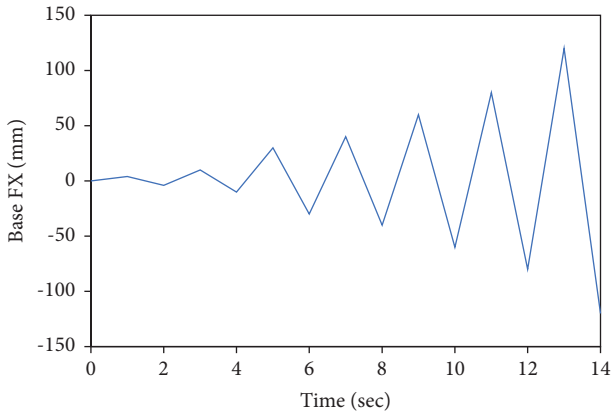

Figure 10: Displacement-based loading protocol.

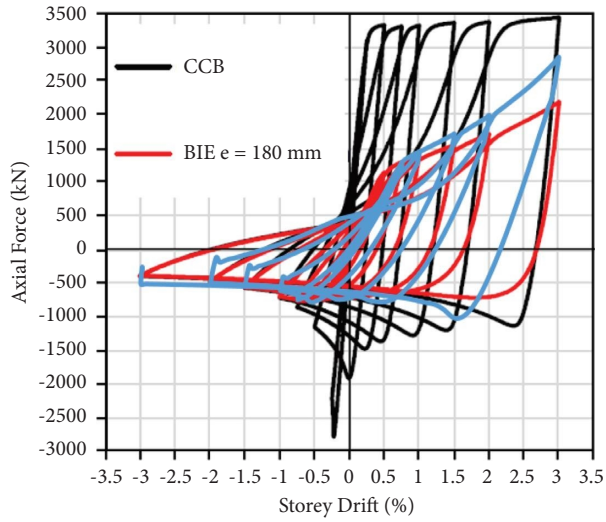

Figure 11: Verification of the load-displacement behaviour of the model in this study with results by González Ureña et al. [12].

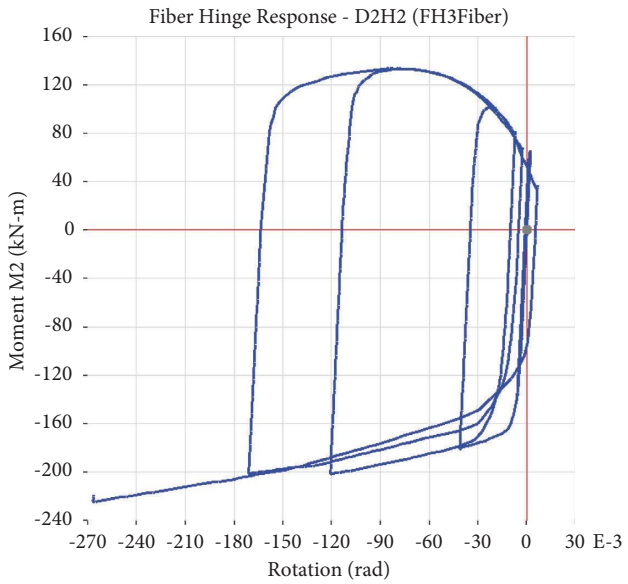

Figure 12: The nonlinear behaviour of the hinge at the middle of the brace.

spectrum for the elastic analysis would be calculated as shown in Figure 15.

3.3. Structural Design. According to the design spectrum obtained in Figure 15, the 20-storey structure is designed in ETABS (for the design details, refer to [17–21]). The cross-sections of the structural elements are shown in Figures 16 and 17.

3.4. BIE System. The same structure designed as EBF is equipped with the BIEs to assess and compare their seismic performance. The same HSS $178 \times 178 \times 16$ sections with

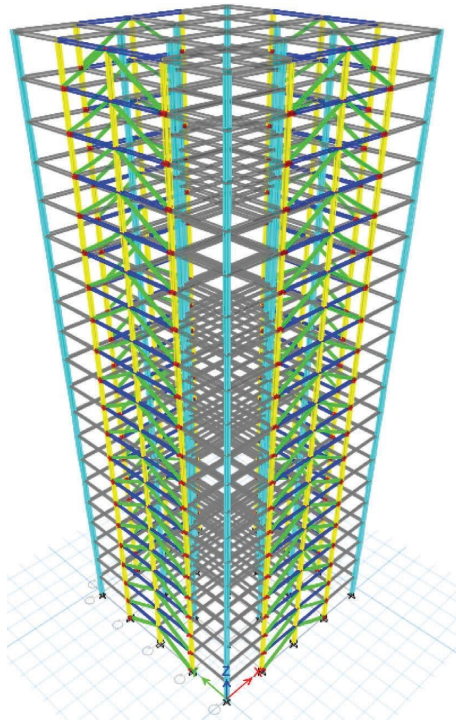

Figure 13: 3D layout of the 20-storey structure with EBF bracing.

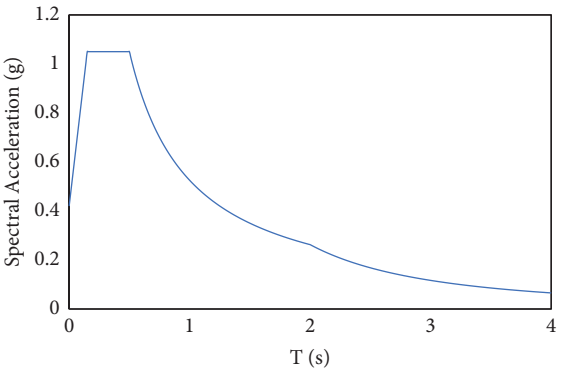

Figure 14: Horizontal elastic response spectrum.

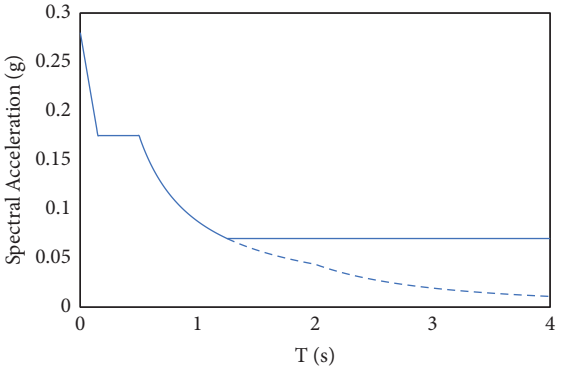

Figure 15: Design spectrum for elastic analysis.

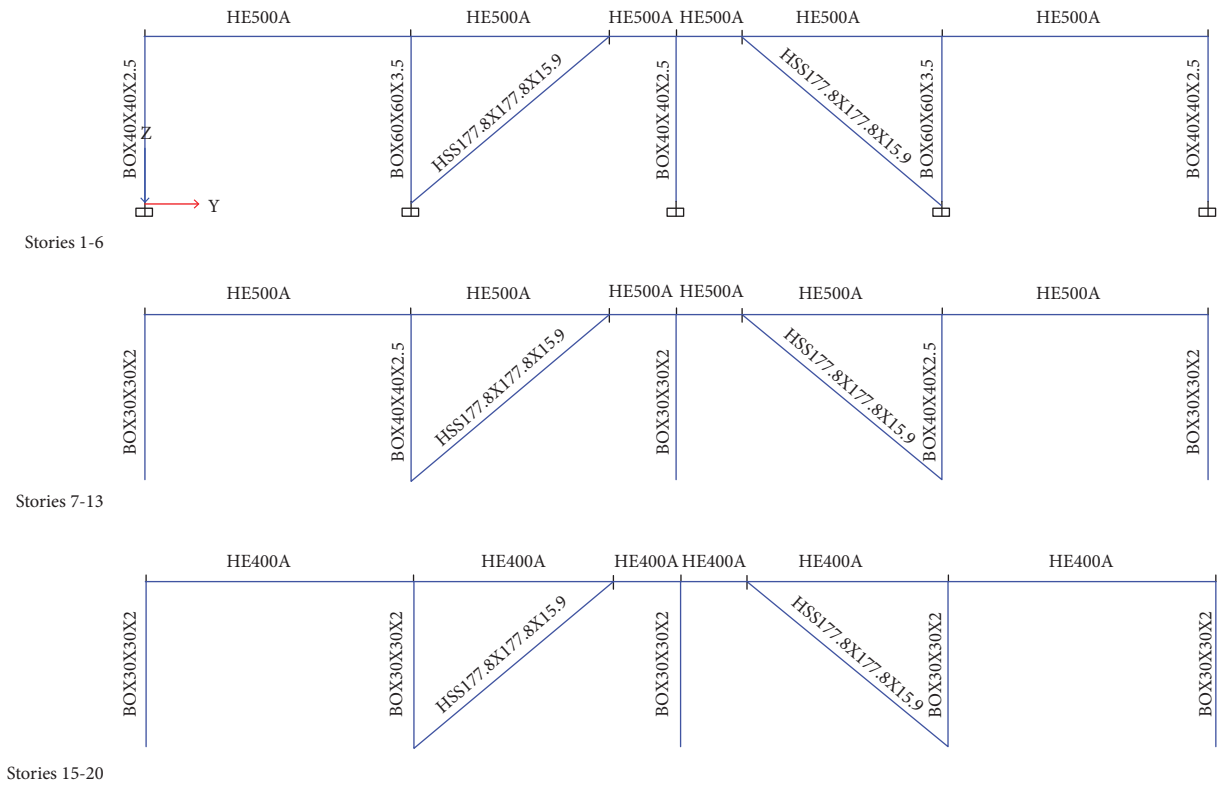

Figure 16: Design sections for outer frames.

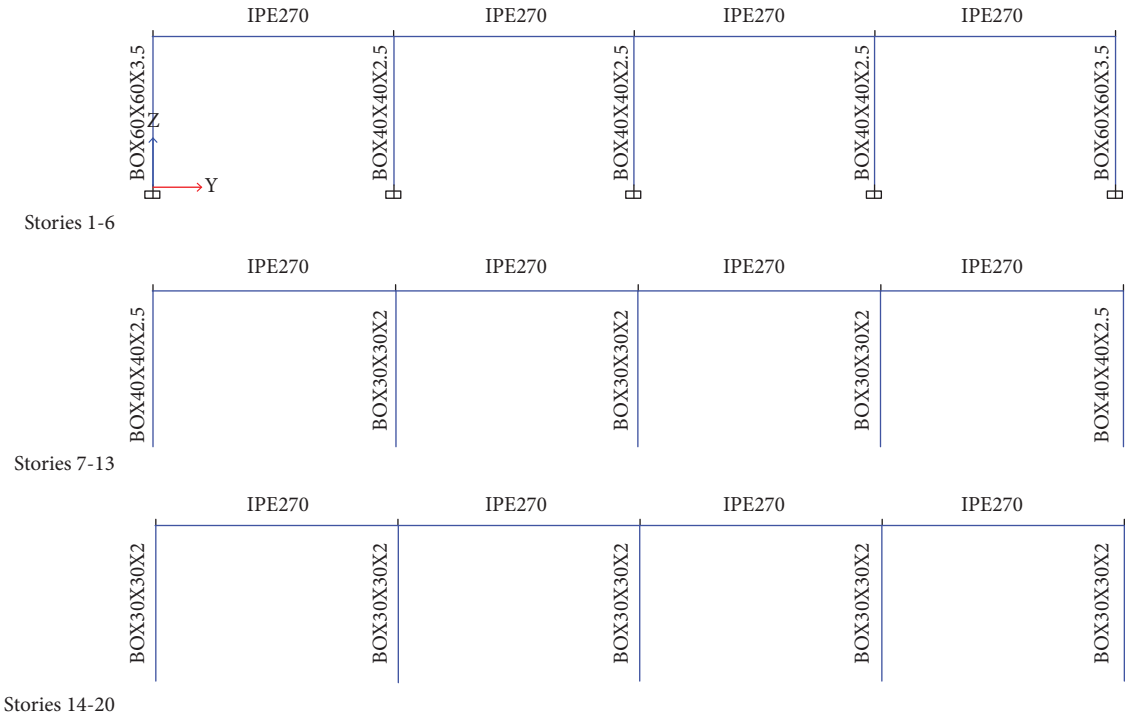

Figure 17: Design sections for inner frames.

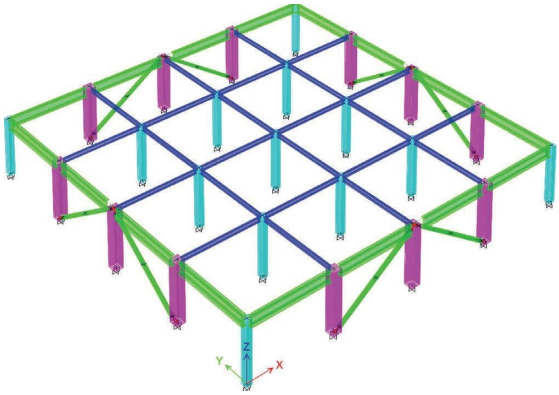

Figure 18: The first storey of the 20-storey structure with BIEs.

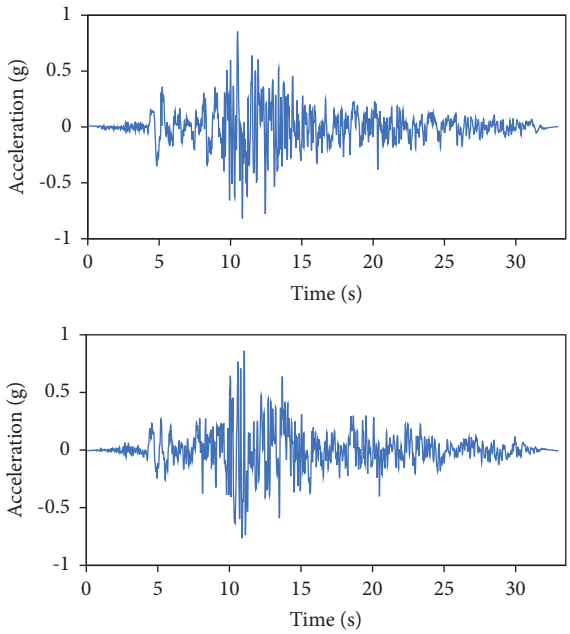

Figure 19: Unscaled accelerogram for the TABAS earthquake RSN143.

120 mm eccentricity are used as BIE members, and the only difference is that smaller cross-sections are used for beams in this structure since bracings are not connected to the beams in the BIE system and there is no need to use heavy beam sections. BIEs are placed in the two middle spans as shown in Figure 18. The details of the installation with rigid elements are shown in Figure 9.

3.5. Nonlinear Time-History Analysis. The nonlinear behaviour of the structure with two bracing systems is investigated under the TABAS earthquake. Its accelerogram is available in the PEER database by RSN143. The two unscaled horizontal components of this record are shown in Figure 19.

This earthquake record should be scaled according to Eurocode 8 [16]. The EC8 recommends that the artificial records should be generated by scaling real ground motion records. For this purpose, the spectrum of the scaled records

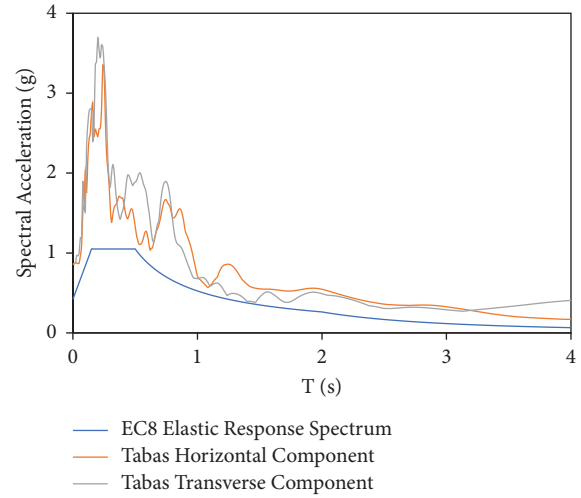

Figure 20: Scaling process of the TABAS accelerogram.

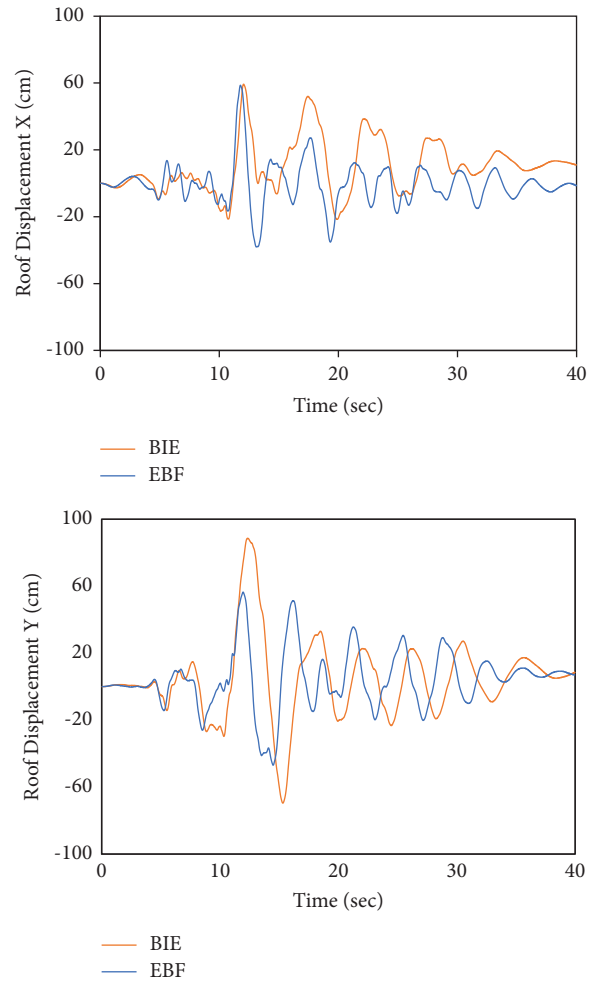

Figure 21: Roof displacement for BIE and EBF structures in X and Y directions.

should be always larger than 90% of the target spectrum in the periods between 0.2 T1 and 2.0 T1. Here, T1 is the fundamental period of the structure in the direction where

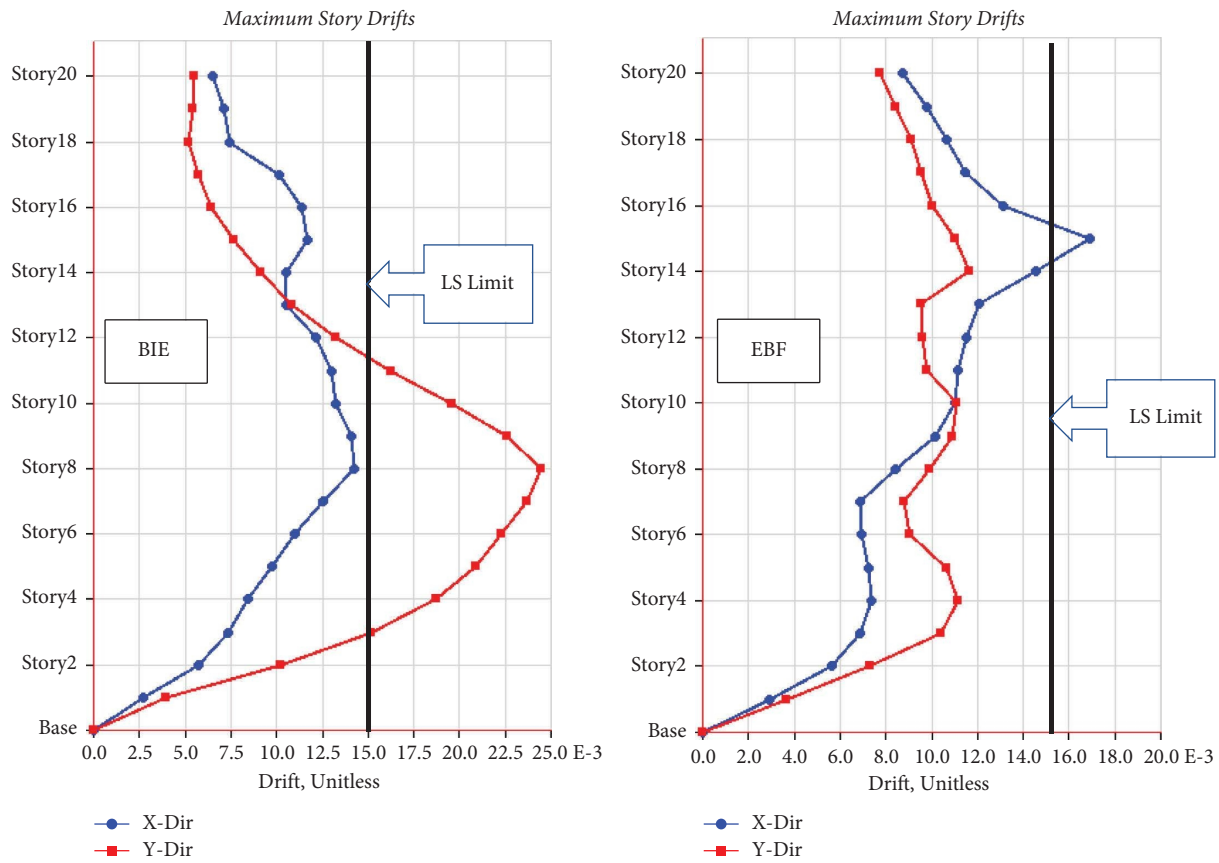

Figure 22: Maximum inter-story drifts along the height of the two structures.

the excitation is applied. Also, the value of the average spectrum at $T1 = 0$ should be larger than the value of the target spectrum at $T1 = 0$. The first mode period of the structure with EBF is 3.1 seconds and for the structure with BIEs is 3.5 seconds. According to Figure 20, a 0.8 scale factor can be used for this earthquake record.

3.6. Seismic Responses. The structural responses of the two systems are compared in this section. Figure 21 shows the roof displacement of the two structures. As displayed in the figure, the displacement in the EBF system is smaller than the displacements in the BIE system by 39% showing the larger stiffness of the EBF system. So, very larger braces should be used in the BIE system to gain an equivalent stiffness, however, we will see in the following sections that this system has acceptable seismic performance and the use of larger braces is not required.

The drift limit for life safety (LS) performance level according to a table in ASCE41-06 (2007) is 0.015. The distribution of maximum drifts along the height of the building is shown in Figure 22. It can be seen that the interstorey drift in the BIE system is larger than the EBF system and the LS level is not satisfied in the BIE system. In order to have a comparison between the two systems, the bracing cross-sections are not changed here. It is obvious that the drift ratios in the BIE system can be reduced by using larger cross-sections and smaller eccentricity.

The plastic hinges developed in BIEs and link beams are shown in Figure 23. It can be seen that the BIE system has provided a uniform distribution of plastic hinges along the height of the structure. Although the lateral rigidity of the structure in the EBF system is larger and the displacement of the structure is smaller in the EBF system, the concentration of damages in plastic hinges is larger in EBF link beams, and it can be verified from Figure 23. The sample hysteresis behaviour of nonlinear hinges for the two systems is shown in Figure 24.

It should be mentioned that in the BIE system, braces show large maximum out-of-plane deformation as shown in Figure 25 for an exterior frame of the structure. These deformations are more than 20 cm in some cases when the members are in compression. This large deformation is due to the geometry of the BIEs as shown in Figure 6. It can be concluded as a disadvantage of the BIE system which may affect the outer facing and claddings of the structure.

The dissipated energy in the BIE system is shown in Figure 26. Also, for the EBF system, it is shown in Figure 27. It can be seen that the dissipated energy in the BIE system (yellow colour) is larger than the EBF system by 160%.

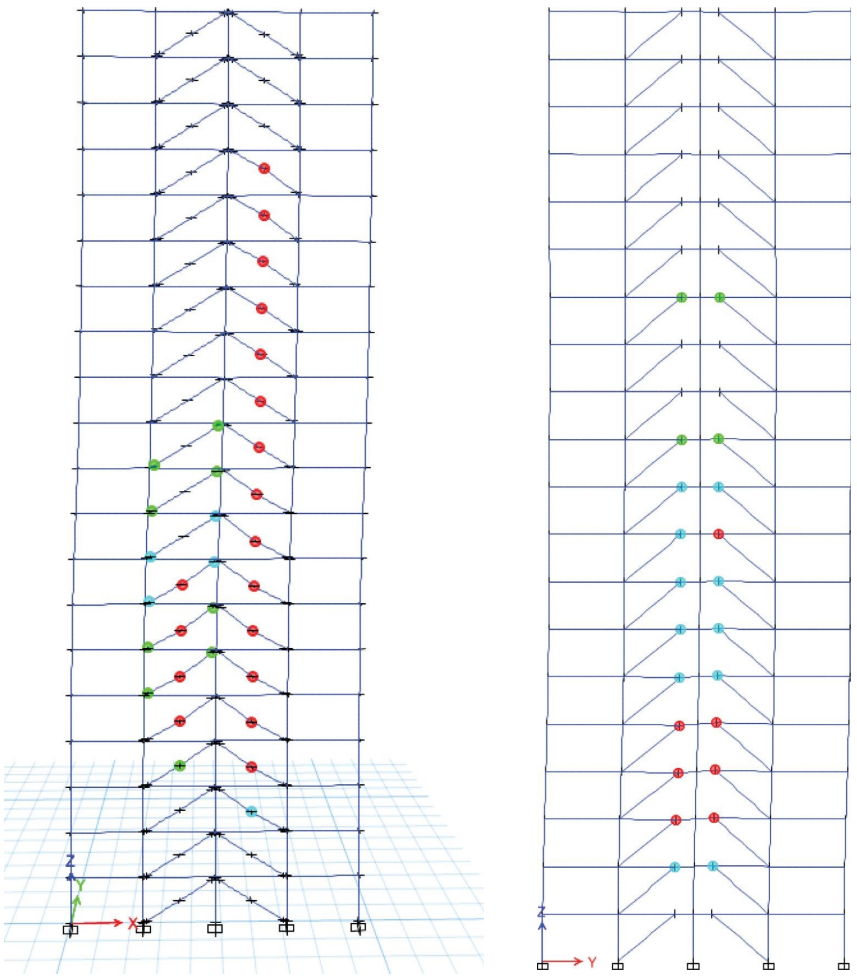

Figure 23: The developed hinges in BIEs and link beams.

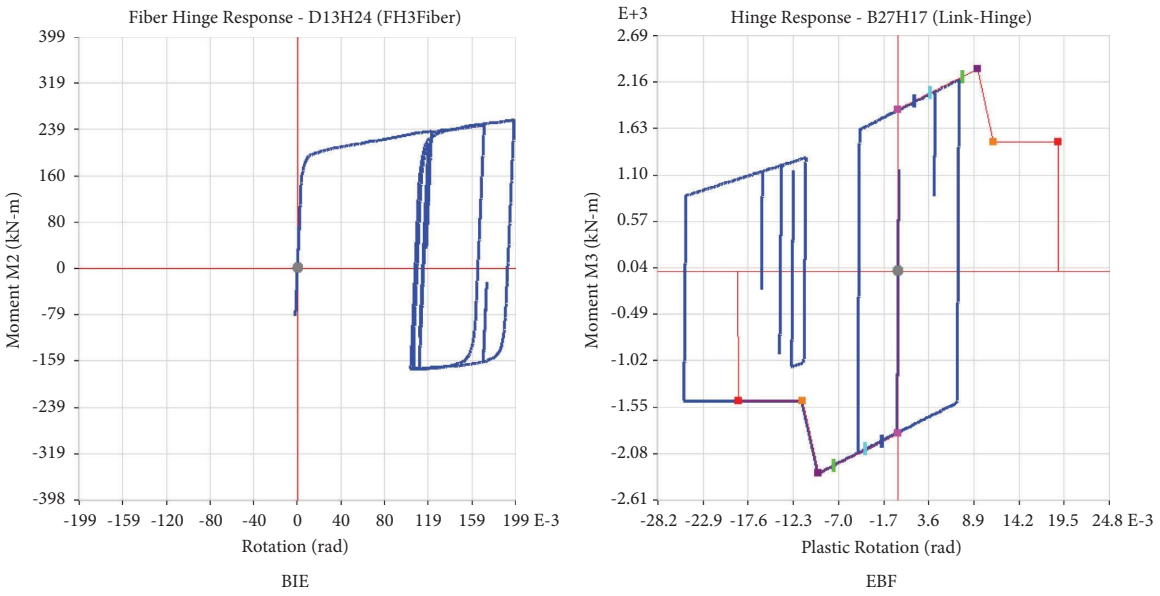

Figure 24: Sample hysteresis behaviour of nonlinear hinges for BIE and EBF systems.

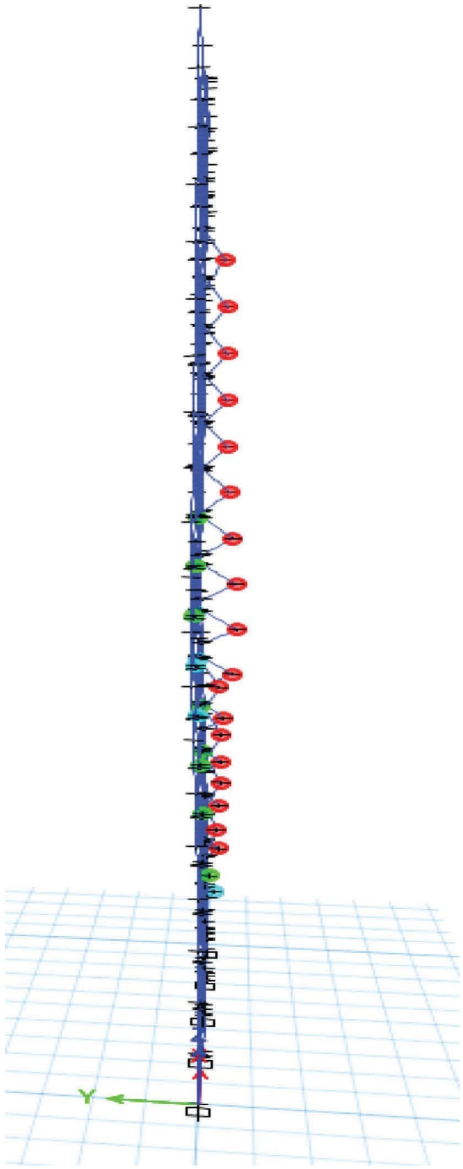

Figure 25: Out-of-plane deformation of braces in the BIE system (horizontal scale is doubled).

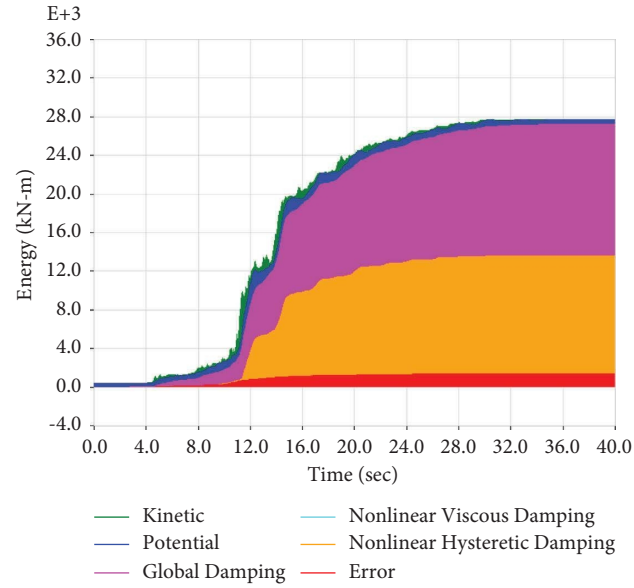

Figure 26: The dissipated energy in the BIE system.

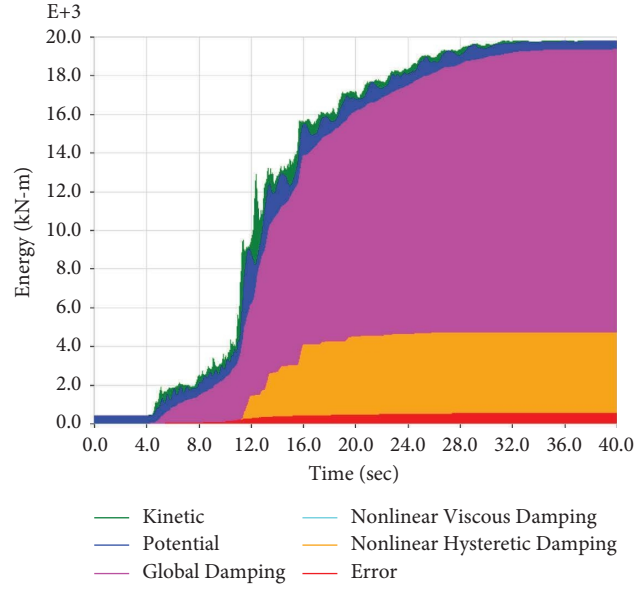

Figure 27: The dissipated energy in the EBF system.

The storey shear forces for the BIE and BF systems are shown in Figure 28. It can be seen that the storey shear forces in the BIE system are less than those in the EBF system. The maximum base shears of the two systems are compared in Table 1.

The steel materials used in the two systems are compared in Table 2. It can be seen that the steel material used in the BIE system is less than the EBF system by almost 20%. This reduction is caused by the smaller beam sections in the BIE system. It is obvious that using larger BIE elements to control the storey drifts may reduce this saving.

4. 25-Storey Structure with Vertical Irregularity

4.1. Structural System. The second structural model for which the seismic performance will be assessed is a 25-storey building with vertical irregularity. This irregularity is in the form of a setback in the 11^{th} and 19^{th} storey of the building. This structure is considered here to assess the performance of BIEs in irregular structures and torsional effects when BIEs are located near the central core of the structure. It is assumed that the building is located in an area with high seismicity. Eurocodes 3 and 8 are used to design the structure. Similar to the previous section, it is assumed that the ground type is B and the seismic zone is 1 with $a_{gr} = 0.35$ g according to [15]. The storey heights are 3.5 m and the bay widths are 6 m. Steel materials are assumed to have a yield stress of 345 MPa. A 3D layout of the frame is shown in Figure 29. Also, the first storey of this structure is shown in Figure 30 to show the location of BIEs. The braces near the core of the structure are placed at all storeys

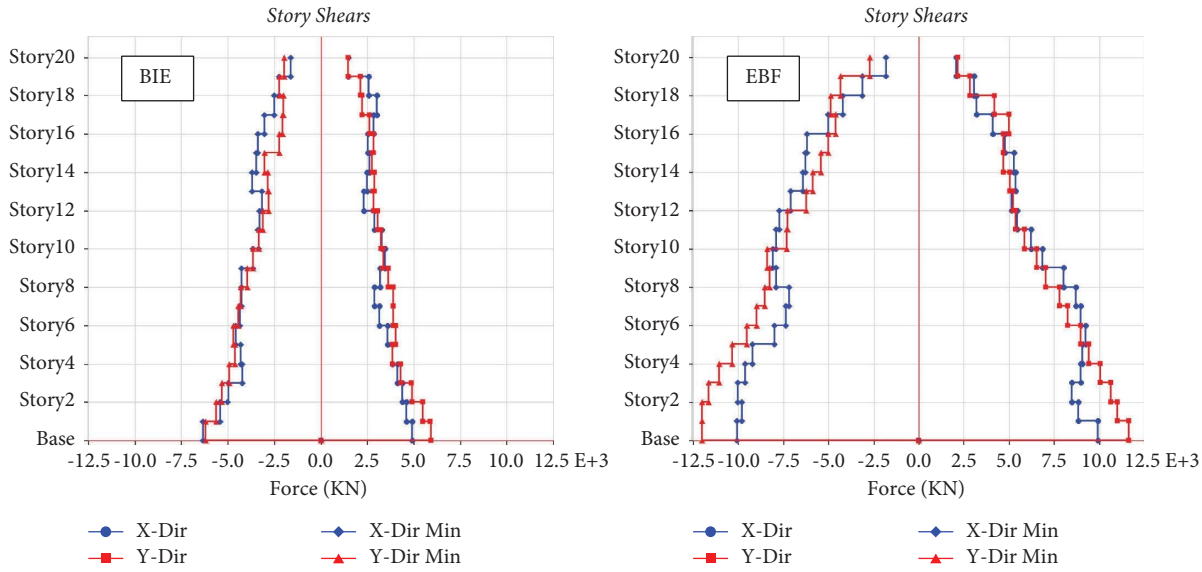

Figure 28: Maximum story shear forces in the 20-story structure with BIE and EBF systems.

Table 1: Base shears in a 20-storey structure with BIE and EBF systems.

System	Base shear	
	EBF (kN)	BIE (kN)
X direction	1043	6432
Y direction	1230	6370

Table 2: Steel material used in the 20-storey structure with BIE and EBF systems.

System	Steel weight	
	EBF (ton)	BIE (ton)
Column	516	516
Beam	385	162
Brace	66	72
Sum	967	750

throughout the height of the structure while the braces at the outer face of the building are continued up to the 10^{th} storey. To highlight the seismic performance of BIEs and their capacity for energy dissipation, all beam to column connections are assumed to be hinged.

4.2. Horizontal Elastic Response Spectrum. Since the location of the buildings studied in this research is constant, the horizontal elastic response spectrum used for this structure is the same as that calculated in previous sections. Therefore, the elastic response spectrum will be in the form of Figure 14. It should be noted that the BIE system is not introduced in the current seismic codes and we have made a rough assumption to design the structure and acquire the cross-sections of the beam and column elements. The value of the behaviour factor is assumed to be $q = 6$, and therefore, the design spectrum for the elastic analysis would be calculated as shown in Figure 15.

4.3. Structural Design. According to the design spectrum obtained, the 25-storey structure is designed in ETABS. The cross-sections of structural elements are shown in Figures 31 and 32. HSS $178 \times 178 \times 16$ sections with 120 mm eccentricity are used as BIE members in this structure. It should be noted that BIEs are not displayed in these figures because they are at another elevation coordinate due to the intentional eccentricity. Instead, their locations are shown in Figure 30.

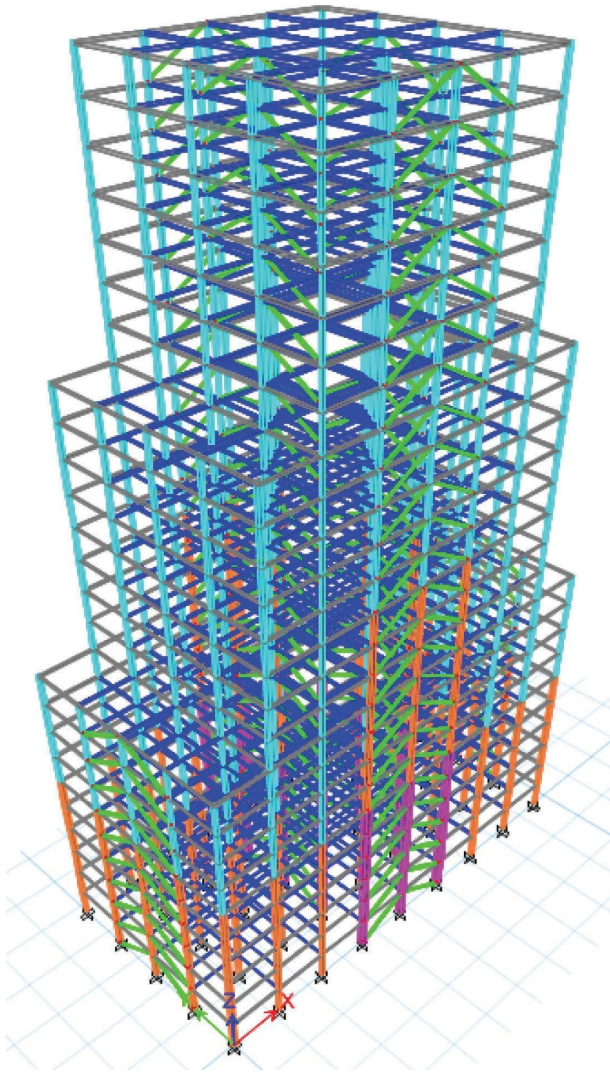

Figure 29: 3D layout of the 25-storey irregular structure with BIEs.

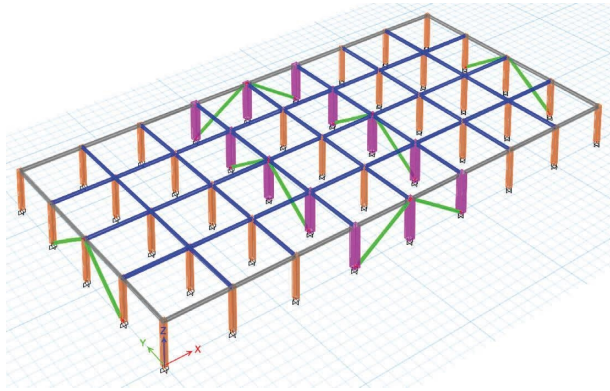

Figure 30: The 1st storey of the 25-storey structure and location of BIEs.

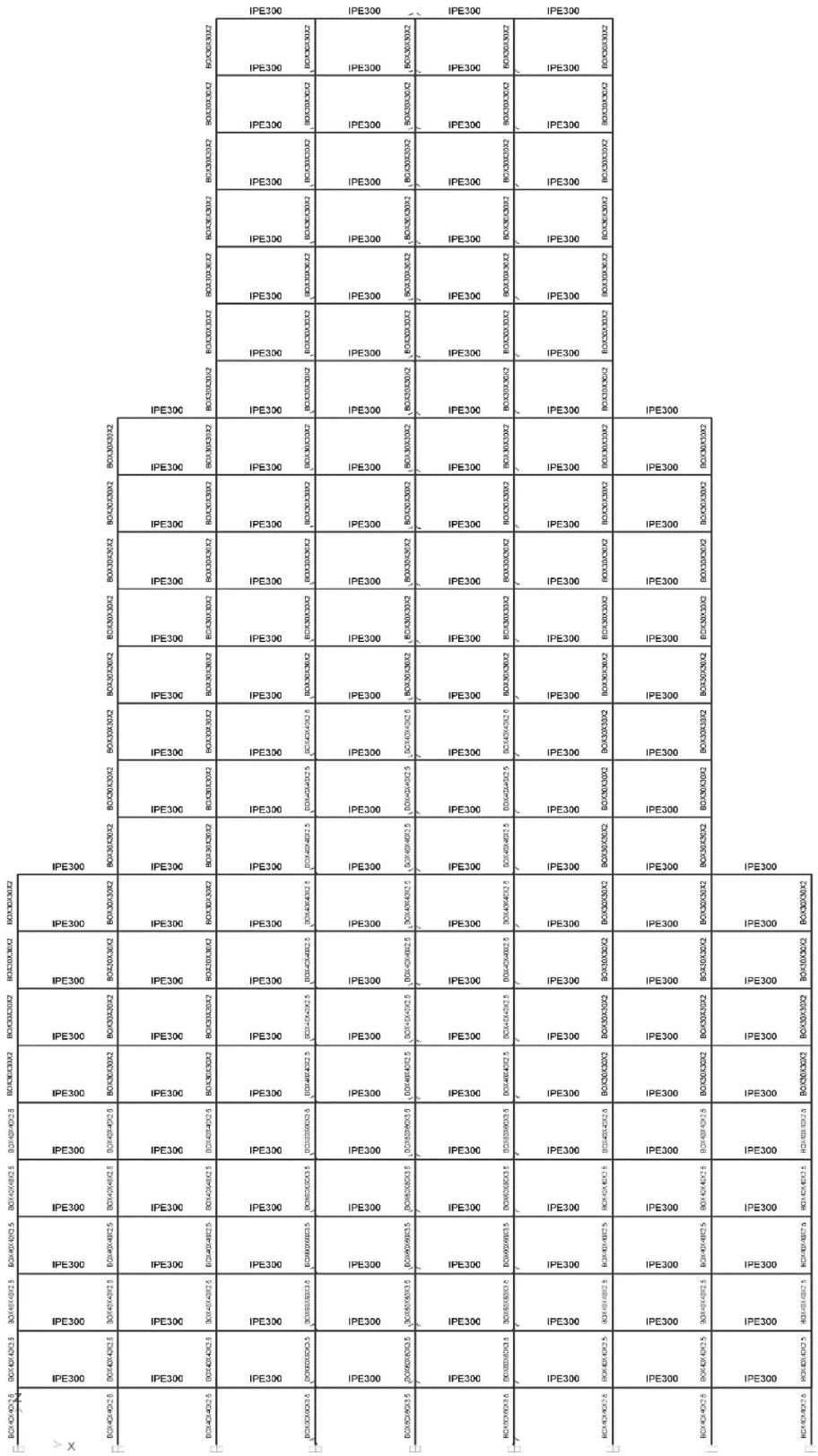

Figure 31: Design sections for outer frames.

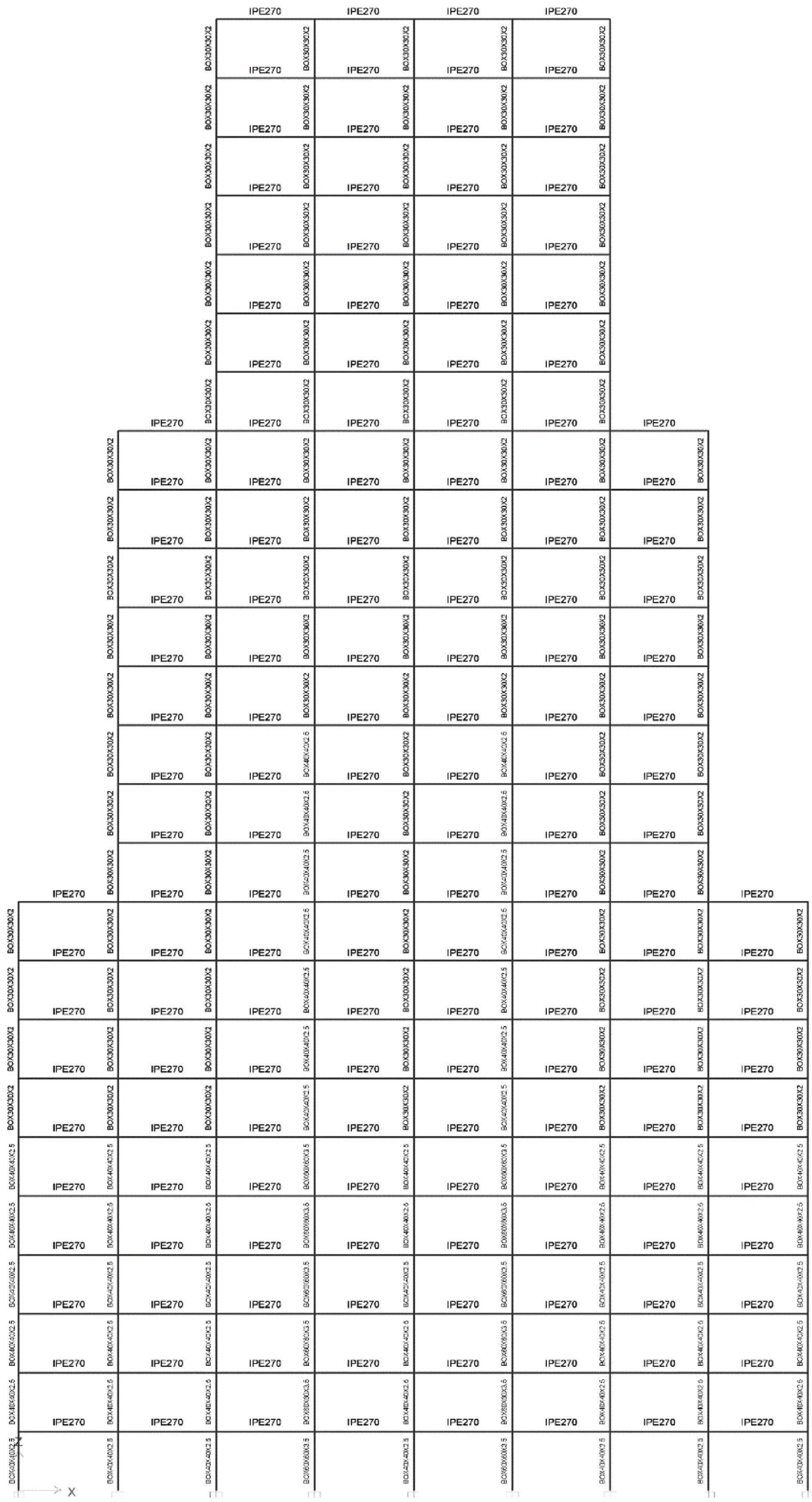

Figure 32: Design sections for inner frames.

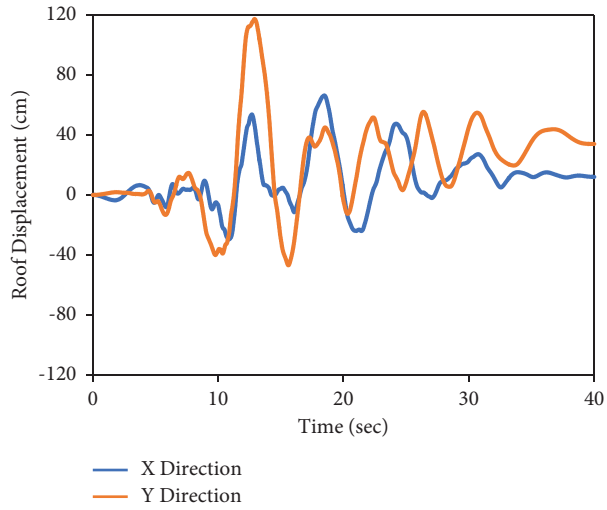

Figure 33: Roof displacement for the 25-story structure with BIEs in X and Y directions.

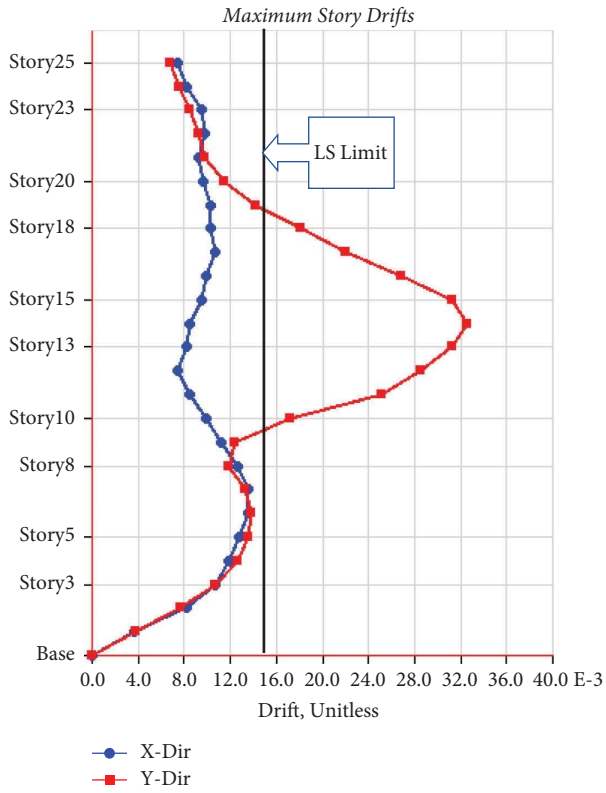

Figure 34: Maximum inter-story drifts along the height of the 25-story structure.

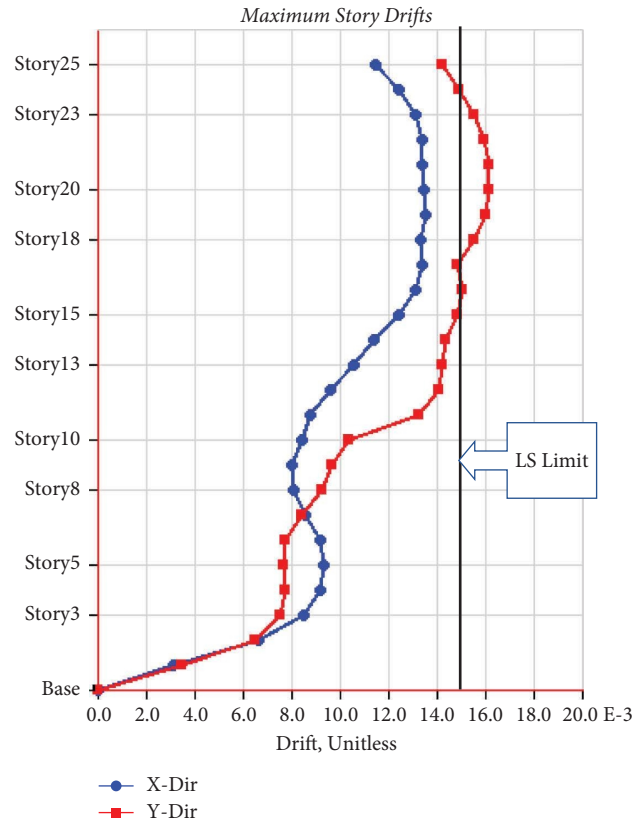

Figure 35: Maximum inter-story drifts along the height of the strengthened 25-story structure.

4.4. Nonlinear Time-History Analysis. Similar to the previous sections, the nonlinear behaviour of the 25-storey structure with vertical irregularity is investigated under the TABAS earthquake. The first mode period of the 25-storey structure with BIEs is 5.5 seconds. According to Figure 20, a 0.8 scale factor can be used for this earthquake record.

4.5. Seismic Responses. The structural response of the structure is examined in this section. Figure 33 shows the roof displacement of the 25-storey structure in both directions. A considerable residual displacement in the order of 40 cm is seen in the Y direction. This may be attributed to the irregularity of the structure. Also, the distribution of maximum drifts along the height of the building is shown in

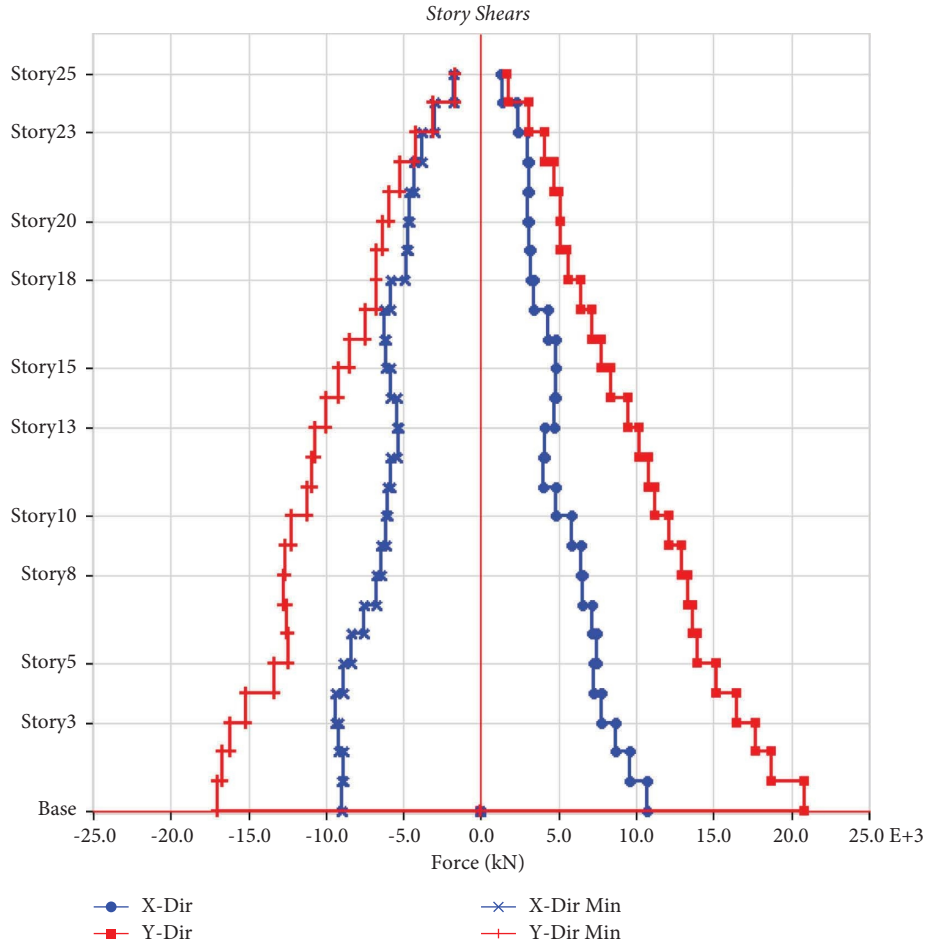

Figure 36: Maximum story shear forces in a 25-story strengthened structure.

Figure 34. Large interstorey drifts are seen in storeys from 10 to 19, where setbacks are applied in the architecture of the building. This issue is very important since the drift values are beyond the Life Safety (LS) limit according to ASCE41-06 (2007) and may cause instability of the structure. The LS limit (0.015) is also displayed in Figure 34.

It can be inferred that the BIEs installed at some storeys are not sufficiently stiff to reduce the storey displacements because of the effects of irregularities, and hence they should be strengthened. The setbacks at the 11^{th} and 19^{th} storey levels cause concentrated storey shears at these storeys. Therefore, larger sections are used as the BIEs in these storey levels which are investigated in the following section.

4.6. Strengthened 25-Storey Structure. Larger BIE sections are used in the y direction of the newly strengthened 25-storey structure (HSS $304 \times 304 \times 16$). Also, the intentional eccentricity is reduced to 80 mm for more rigidity. The effect of reducing the intentional eccentricity on the maximum storey drifts and also on the energy dissipation capacity of the BIE system may be verified here. The first mode period (T_1) of this structure is reduced to 4.5 seconds. It is worth mentioning that the scale factor for the earthquake record remains unchanged since the governing part of the response spectrum is at about 1.5 seconds.

The abovementioned strengthening has resulted in less interstorey drifts as shown in Figure 35. It can be seen that the LS performance level is mostly satisfied in this structure and the maximum drift ratios are reduced by almost 50%. By a trial-and-error procedure, an appropriate rigidity and strength of the structure can be achieved by selecting a proper cross-section of BIEs and proper eccentricity while maintaining the energy-dissipating capacity of the structure. It is a considerable advantage of the BIE system.

The maximum storey shear forces are shown in Figure 36. A uniform distribution of the shear forces is seen in this Figure 36. Larger sections and less eccentricity of BIEs in the y direction have resulted in larger shear forces in the y direction.

The plastic hinges developed in BIEs are shown in Figure 37. It can be seen that the BIE system has provided a uniform distribution of plastic hinges along the height of the structure up to the 14^{th} storey.

Similar to the 20-storey structure, large out-of-plane deformations in BIEs are seen. These deformations are more than 30^{cm} in some cases.

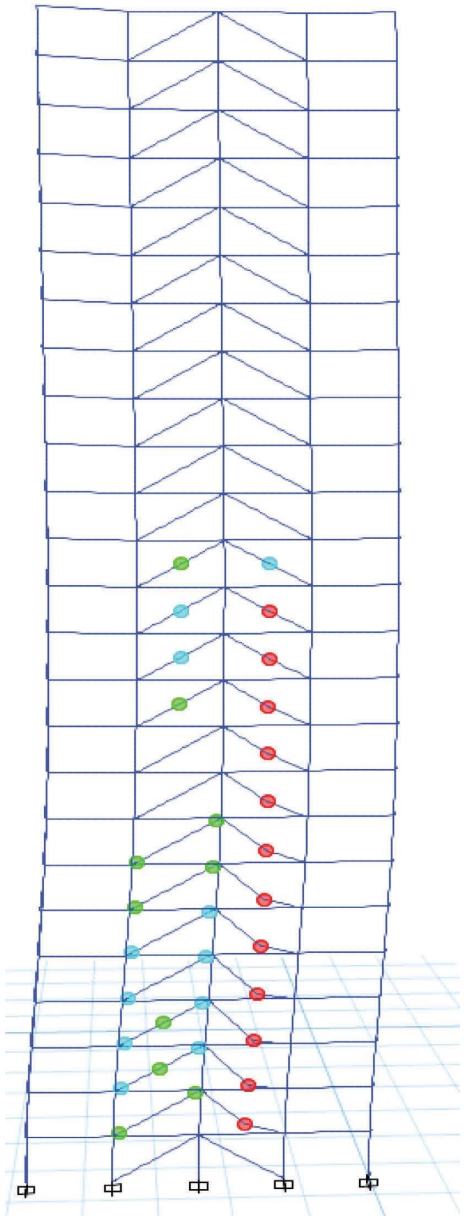

Figure 37: The developed hinges in BIEs and link beams.

The dissipated energy in the BIE system is shown in Figure 38. The yellow part shows the energy dissipated by BIEs.

In order to investigate the torsional effects in the irregular structure, the max/average values of storey drifts are checked. This ratio is under 1.2 for all storey levels.

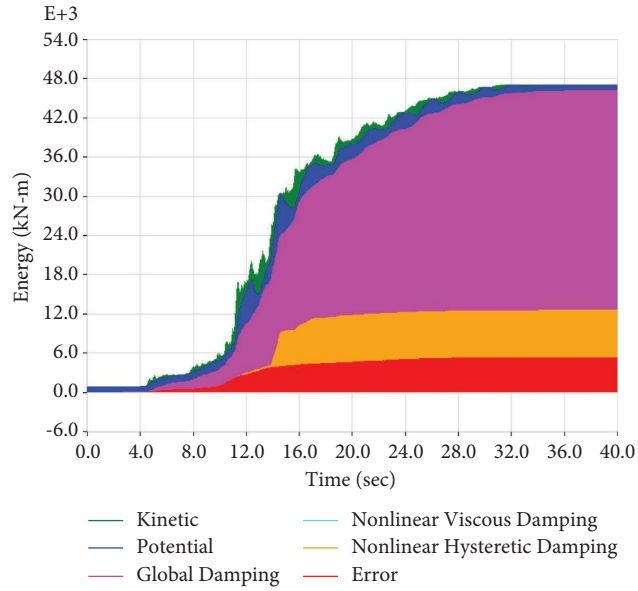

Figure 38: The dissipated energy in the BIE system for the strengthened 25-story building.

Therefore, no excessive torsional displacement is induced in this structure under seismic excitation.

5. Conclusions

In previous sections, an analytical assessment of the seismic performance of structures with the BIE system was carried out. Since the cyclic behaviour of BIEs is the main aspect of these bracing systems which affects the global behaviour of the structure under seismic loadings, as the first step, a proper model of the BIE was developed in ETABS. This model was verified by the results from previous studies to attain a proper estimate of the BIE's cyclic behaviour and backbone curve. In the second step, a 20-storey regular structure was designed by the EBF system and then, in the same structure, the bracings were replaced by BIEs. The seismic performance of the two structures was compared under the TABAS earthquake record in terms of roof displacement, storey drift ratios, dissipated energy, and steel weight. In the third step, the seismic performance of a 25-storey irregular structure was examined. The irregularity was in the form of a setback in the 11^{th} and 19^{th} storey of the building. The interstorey drift ratios in this structure were verified with the LS performance level, and the structure was strengthened to achieve this performance level under the TABAS earthquake record. According to the results

obtained in previous sections, the following conclusions may be derived:

(1) The verification of the behaviour of the developed model by comparing the load-displacement diagrams generated by González Ureña et al. [12] with the results of the generated model in this study showed that the developed model succeeds in providing good estimates of the compressive and tensile behaviour of BIE. The results showed that a combination of the three fiber hinges (two at both ends and one at the middle of the element) and one axial hinge in a BIE element will result in a proper numerical model of the BIE members.

(2) According to the results obtained for the 20-storey structure, the BIE system provides less lateral stiffness compared to the EBF system, resulting in larger lateral displacements and drifts. Larger cross-sections should be used in BIE elements to satisfy drift limits according to design codes.

(3) The BIE system provides a uniform distribution of plastic hinges along the height of the structure preventing the concentration of damages in plastic hinges. The plastic hinges in the BIE system develop at the initial stages of seismic excitation thus providing a good energy dissipation capacity.

(4) Stable hysteresis behaviour is seen in the BIE system resulting in a large amount of energy dissipation compared to the EBF system. BIEs start to dampen and dissipate input energy from the early levels of excitation.

(5) The fraction of dissipated energy in the BIE system was much larger than that of the EBF system. This fraction is calculated relative to the total input energy. This shows the superiority of the BIE system in energy dissipation capacity.

(6) Comparison between storey shear forces in the two structures with the BIE and EBF systems showed that the BIE system was subjected to less storey shear forces. This may be partly due to the less rigidity of the BIE system. However, a comprehensive conclusion requires further investigations comparing the seismic shear forces in the two systems with the same storey yield shears.

(7) In the BIE system, braces showed large out-of-plane deformation. These deformations are more than 20 cm in some cases which can be considered as a disadvantage of the BIE system.

(8) A comparison of the steel material weight of the two 20-storey structures with the BIE and EBF systems showed that the steel material in the structure with the BIE system is almost 20% less than the EBF system. This reduction is caused by the smaller beam sections in the BIE system. It is obvious that using larger BIE elements to control the storey drifts may reduce this saving.

(9) The performance assessment of the 25-storey irregular structure showed a considerable residual displacement in the order of 40 cm in the Y direction. This may be attributed to the irregularity of the structure.

(10) Large interstorey drifts were seen in storeys from 10 to 19 of the 25-storey structure before strengthening where setbacks were applied in the architecture of the building. The drift values were beyond the life safety (LS) limit according to ASCE41-06. To overcome this shortcoming, the 25-storey structure was strengthened by using larger sections and less intentional eccentricities in BIEs.

(11) The strengthening (larger sections and less intentional eccentricities of BIEs) applied on the 25-storey structure resulted in reduced interstorey drifts by almost 50%. By a trial-and-error procedure, an appropriate rigidity and strength of the structure can be achieved by selecting a proper cross-section of BIEs and proper eccentricity while maintaining the energy-dissipating capacity of the structure. It is a considerable advantage of the BIE system.

(12) In order to investigate the torsional effects in the structures with vertical irregularity, the max/average values of the storey drifts were explored. The ratio obtained at all storey levels was less than 1.2. Therefore, no excessive torsional displacement was induced in an irregular 25-storey structure under seismic excitation.

Data Availability

The data used to support the findings of this study are available from the corresponding author upon request.

Disclosure

This research was performed as part of Master project of the first author under the supervision of the second author in the City, University of London.

Conflicts of Interest

The authors declare that they have no conflicts of interest.

References

[1] F. Fu, *Advanced Modelling Techniques in Structural Design*, John Wiley & Sons, Hoboken, NJ, USA, 2015.

[2] E. J. Lumpkin, P. C. Hsiao, C. W. Roeder et al., "Investigation of the seismic response of three-storey special concentrically braced frames," *Journal of Constructional Steel Research*, vol. 77, pp. 131–144, 2012.

[3] T. Okazaki, D. G. Lignos, T. Hikino, and K. Kajiwara, "Dynamic response of a chevron concentrically braced frame," *Journal of Structural Engineering*, vol. 139, no. 4, pp. 515–525, 2013.

[4] J.-W. Lai and S. A. Mahin, "Steel concentrically braced frames using tubular structural sections as bracing members: design, full-scale testing and numerical simulation," *International Journal of Steel Structures*, vol. 14, no. 1, pp. 43–58, 2014.

[5] F. Fu, *Design and Analysis of Tall and Complex Structures*, Butterworth-Heinemann, Oxford, United Kingdom, 2018.

[6] L. Ye, "Study on the influence of post-yielding stiffness to the seismic response of building structures," in *Proceedings of the Fourteenth World Conference On Earthquake Engineering*, Shanghai, China, June 2008.

[7] M. Baiguera, G. Vasdravellis, and T. L. Karavasilis, "Dual seismic-resistant steel frame with high post-yield stiffness energy-dissipative braces for residual drift reduction," *Journal of Constructional Steel Research*, vol. 122, pp. 198–212, 2016.

[8] H. Iemura, Y. Takahashi, and N. Sogabe, "Two-level seismic design method using post-yield stiffness and its application to unbonded bar reinforced concrete piers," *Structural Engineering/Earthquake Engineering*, vol. 23, no. 1, pp. 109–116, 2006.

[9] D. B. Merczel, "On the weak storey behaviour of concentrically braced frames," in *Proceedings of the 8th International Conference on Behavior of Steel Structures in Seismic Areas STESSA*, Timisoara, Romania, May 2015.

[10] K. A. Skalomenos, H. Inamasu, H. Shimada, and M. Nakashima, "Development of a steel brace with intentional eccentricity and experimental validation," *Journal of Structural Engineering*, vol. 143, no. 8, Article ID 04017072, 2017.

[11] K. A. Skalomenos, M. Kurata, H. Shimada, and M. Nishiyama, "Use of induction-heating in steel structures: material properties and novel brace design," *Journal of Constructional Steel Research*, vol. 148, pp. 112–123, 2018.

[12] A. González Ureña, R. Tremblay, and C. A. Rogers, "Earthquake-resistant design of steel frames with intentionally eccentric braces," *Journal of Constructional Steel Research*, vol. 178, Article ID 106483, 2021.

[13] K. A. Skalomenos, H. Shimada, M. Kurata, and M. Nakashima, "03.03: feasibility of hybrid simulation for testing steel connections of braces with intentional eccentricity," *Ce/Papers*, vol. 1, no. 2-3, pp. 522–529, 2017.

[14] K. A. Skalomenos, M. Kurata, and M. Nishiyama, "Induction-heat treated steel braces with intentional eccentricity," *Engineering Structures*, vol. 211, Article ID 110461, 2020.

[15] G. Solomos, "A Review of the Seismic hazard Zonation in National Building Codes in the Context of Eurocode 8," *JRC Scientific and Technical reports*, International Space University, Illkirch-Graffenstaden, France, 2008.

[16] BSI, *Eurocode 8: Design of Structures for Earthquake Resistance-Part 1: General Rules, Seismic Actions and Rules for Buildings*, European Committee for Standardization, Brussels, Belgium, 2005.

[17] K. Qian, D. Q. Lan, F. Fu, and B. Li, "Effects of infilled wall opening on load resisting capacity of RC frames to mitigate progressive collapse risk," *Engineering Structures*, vol. 223, Article ID 111196, 2020.

[18] K. Qian, S. Liang, F. Fu, and Y. Li, "Progressive collapse resistance of emulative precast concrete frames with various reinforcing details," *Journal of Structural Engineering*, vol. 147, no. 8, Article ID 04021107, 2021a.

[19] K. Qian, S. L. Liang, F. Fu, and Y. Li, "Progressive collapse resistance of emulative precast concrete frames with various reinforcing details," *Journal of Structural Engineering*, vol. 147, no. 8, Article ID 05021004, 2021b.

[20] F. Fu, D. Lam, and J. Ye, "Modelling semi-rigid composite joints with precast hollowcore slabs in hogging moment region," *Journal of Constructional Steel Research*, vol. 64, no. 12, pp. 1408–1419, 2008.

[21] F. Fu, D. Lam, and J. Ye, "Moment resistance and rotation capacity of semi-rigid composite connections with precast hollowcore slabs," *Journal of Constructional Steel Research*, vol. 66, no. 3, pp. 452–461, 2010.